Machine learning based Computer-Aided Diagnosis of liver tumours

Liaqat Ali[1], Khaled Khelil[2], Summrina K. Wajid[1], Zain U. Hussain[3], Moiz A. Shah[4], Adam Howard[5], Ahsan Adeel[1], Amir A. Shah[6], Unnam Sudhakar[6], Newton Howard[7], Amir Hussain[1]

[1] School of Natural Sciences, University of Stirling, Stirling, FK9 4LA; [2] Electrical Engineering Department, University of Souk Ahras, Algeria; [3] University of Edinburgh, Edinburgh, UK; [4] University of Glasgow, Glasgow, UK; [5] Brown University, USA; [6] Kilmarnock NHS Hospital, Scotland, UK; [7] Medical Sciences Division, Nuffield Department of Surgical Sciences, University of Oxford, Oxford, UK

Email: [1] {lal, skw, aad, ahu}@cs.stir.ac.uk; [2] k_khelil@yahoo.fr; [3] s1791832@sms.ed.ac.uk; [4] 2015278s@student.gla.ac.uk; [5] howard.adam3@gmail.com; [6] {amir.shah, s.unnam}@aaaht.scot.nhs.uk; [7] newton.howard@nds.ox.ac.uk

Abstract – **Image processing plays a vital role in the early detection and diagnosis of Hepatocellular Carcinoma (HCC). In this paper, we present a computational intelligence based Computer-Aided Diagnosis (CAD) system that helps medical specialists detect and diagnose HCC in its initial stages. The proposed CAD comprises the following stages: image enhancement, liver segmentation, feature extraction and characterization of HCC by means of classifiers. In the proposed CAD framework, a Discrete Wavelet Transform (DWT) based feature extraction and Support Vector Machine (SVM) based classification methods are introduced for HCC diagnosis. For training and testing, the recorded biomarkers and the associated imaging data are fused. The classification accuracy of the proposed system is critically analyzed and compared with state-of-the-art machine learning algorithms. In addition, laboratory biomarkers are also used to cross-validate the diagnosis.**

Keywords: Hepatocellular carcinoma (HCC), Computational Intelligence, Machine Learning, Computer aided diagnosis (CAD), Wavelet Transform (WT), Support Vector Machines (SVM)

I. INTRODUCTION

HCC is the most common form of liver cancer, mainly caused by cirrhosis of the liver secondary to hepatitis infection [1]. At present, around 60% of liver tumors are diagnosed at a later stage with a median survival of ~6 months, whilst those detected early have a 5-year survival rate of 70%. It has recently been evidenced that late detection could be attributed to an absence of detection, despite the use of ultrasound and tumor markers [2]. Multi-Detector-Row-Computed Tomography (MDCT) is the most commonly used diagnosis method by radiologists for detecting HCC. However, due to grey-scale intensity factors, invasive procedures are often resorted to for diagnosis confirmation. The main aim of this research is to develop an intelligent, robust and automated multimodal CAD framework, using state of art machine learning algorithms, wavelet-based features and lab markers. The proposed CAD framework can diagnose liver tumors, accurately, precisely, and at early stages without the use of unnecessary and costly invasive procedures.

The remainder of this paper is organized as follows: Section-II provides an overview of literature in this area work. In Section-III, the proposed CAD design is presented and compared with existing methods. Section-IV explains the experimental results with critical analysis. Finally, the conclusions are presented in Section V and provide a summary of the results, as well as additional information related to HCC.

II. RELATED WORK

In the literature, researchers have proposed several analytical, image processing or machine learning based diagnosis methods for HCC diagnosis, ranging from image enhancement, image segmentation, feature extraction, to classification. For example, the authors in [3] proposed a disk-shaped mask method to carry out Top-Hat and Bottom-Hat transformations for image enhancement. The authors in [4] proposed an object based image contrast stretching method which works by firstly finding the edges of the image Then, the morphological watershed and region growing methods work to segment the images into various objects and divide them into foreground/background regions respectively. After these processes, the authors apply the contract stretching to each region and convert the original image into an enhanced image. The authors also proposed another method which involves merging clipped and non-linear binning, based on a k-means clustering algorithm. This method modifies the amount and distribution of grey levels in order to bring out the fine details of the image and reduce noise. The results interestingly showed that the contrast of the CT image soft tissues was significantly enhanced. The authors in [5] proposed a contrast based method to reduce noise. The proposed method was comprised of image pre-processing for identifying regions of interest and increasing pixel contrast. Simulated results showed that noise was reduced three-fold.

Similarly, in the context of image segmentation, the authors in [6] proposed an Active Contour Model (ACM) based liver segmentation approach. In this method, the authors first extracted the initial contours, and then generated the optimum parameters for ACM. Finally, to refine the initial contour, the authors carried out ACM. The authors in [7] proposed an automatic liver and tumour segmentation using a statistical-parameter-based approach. In this method, the authors first distinguished the liver from other organs. In the second phase, a median filter is applied to remove noise, following the application of threshold, post-processing, reconstruction and statistical parameter methods. The authors in [8] proposed an Artificial Bee Colony (ABC) optimization algorithm to segment the liver. In this method, a clustering technique is applied to segment the liver from the abdominal CT image. The smallest distance is calculated between every pixel value, different centroids are selected in a binary image for each cluster and some

Proc. 2017 IEEE 16th Int'l Conf. on Cognitive Informatics & Cognitive Computing (ICCI*CC'17)
N. Howard, Y. Wang, A. Hussain, F. Hamdy , B. Widrow & L.A. Zadeh (Eds.)
978-1-5386-0771-8/17/$31.00 ©2017 IEEE

morphological operations are applied to every binary clustered image to remove small and thin objects. The authors in [9] proposed a kernel-based extreme learning machine method for automatic liver tumour detection and for semi-automatic segmentation from CT liver images. The results were promising but the data set was limited, with data for only 7 patients.

Similarly, in the context of feature extraction, the authors in [10] proposed an empirical wavelet transform method. Here, correntropy features are extracted using fundus images. They obtained 93.33% accuracy using SVM as the classifier. The authors in [11] proposed a reconstructed wavelet decomposition coefficients method to extract the signals of each frequency. Furthermore, Decomposed Reconstructed Signals (DRS) from low-frequency coefficients and high-frequency coefficients were articulated. The authors in [12] proposed Grey Level Texture (GLT) Features, Wavelet Coefficient Texture (WCT) Features and Contourlet Coefficient Texture (CCT) Features methods and simulations, and demonstrated promising results. The authors in [13] proposed first order statistics, a spatial grey level dependence matrix, a grey level difference method, Laws' texture energy measures, and fractal dimension methods to extract five different feature sets. A further treatment plan for the patient was then based on the classification of the tumour, benign or malignant.

In the context of classification, the authors in [14] proposed an automated classification method to distinguish between lung surfaces. Here, the line of pleurae surrounding the reflection of the lung are automatically detected and the surface is divided into smaller sections. Further, rules are automatically generated by C4.5 and Ripple-Down Rules (RDR) for classification. The experiment was robust and showed high accuracy (92%) in 808 test cases. The authors in [15] proposed Support Vector Machines (SVM) with a kernel-based supervised learning method, however the simulation and results were not significant.

Although there has been much research and discussion on HCC detection, diagnosis and classification, there are still numerous limitations, as identified above. Studies were often inaccurate in diagnosing HCC, and computational performance tends to be poor. To address these issues, there is a need for the development of a state-of-the-art, computationally intelligent and fully automated CAD system which can accurately segment, extract and classify HCC. This paper proposes a computational intelligence based, fully automated, HCC detection, diagnosis and classification CAD system.

III. Proposed Computational Intelligence CAD System

The proposed CAD system consists of the following four stages: 1) Image enhancement, 2) Image Segmentation, 3) Wavelet Transform Feature extraction, and 4) Lab marker and image features fusion, and followed by 6) Classification. The overall structure of the proposed CAD framework is shown in Figure 1.

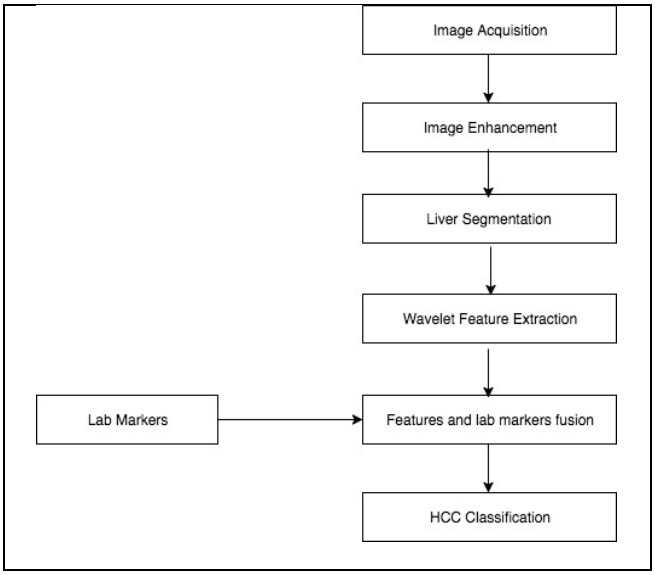

Fig. 1. Proposed CAD Framework

The major contributions of this work include: (1) The novel formulation of a wavelet transformation model to extract HCC features from CT images, and (2) The enhanced classification of such features, using CT images. Prior to the extraction of HCC features, the liver region was first automatically segmented from the CT image [16] and its features were then extracted from the size of the three-dimensional array plane using discrete wavelet transform. The coefficient matrices were generated for the approximation of horizontal, vertical and diagonal details. The fusion of the imaging data and the associated lab markers were both used for cross-validation of the HCC diagnosis and served as input for training and testing the machine-learning-based classification.

A. *Image Enhancement*

We introduced applied Contrast Limited Adaptive Histogram Equalization (CLAHE) [17] for image enhancement. This approach has gained reasonable popularity and is now frequently used to enhance medical images. An image is firstly divided into contextual blocks and then applies Histogram Equalization to the sub-regions of each block of an image. Later, a histogram for each block is generated using a specific number of bins and the histogram is clipped at a certain threshold, according to the new histogram results. Finally, a grey level [12] enhanced image ready for Region-Of-Interest (ROI) segmentation is interpolated. Furthermore, we compared and evaluated the qualitative and quantitative performance of state of art image enhancement algorithms. The following steps were followed to enhance the CT image:

- Load CT image
- Convert RGB image into grayscale image
- Carry out Contrast adjustment function to equalize the image pixel intensity
- Apply contrast limiter adaptive histogram equalization method for histogram equalization
- Restore better quality enhanced image

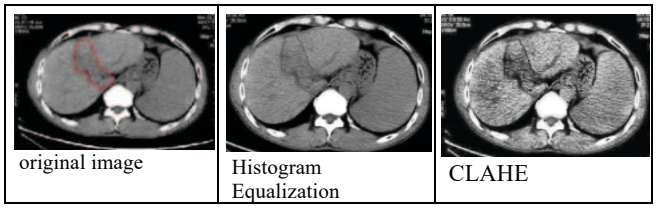

Fig. 2. Image enhancement results

B. *Liver Segementation*

We presented an efficient, automatic liver detection and segmentation that is based on morphological operations with 3-D CT scan images [16]. Automatic liver segmentation was carried out as follows:

a) Apply masking and prediction to visualize the maximum area of the liver.
b) Define and calculate the liver area based on the shape and prior knowledge.
c) Morphological operations are then carried out to segment the liver from the rest of the organs, which are removed by morphological erosion and result in an isolated liver region.
d) Apply a low pass Gaussian filter (**G**(.)) to remove noise and preserve the edges.

$$\boldsymbol{G(x,y) = \frac{1}{\sqrt{2\pi\sigma}} \exp\left(-\frac{x^2+y^2}{2\sigma^2}\right)} \quad \textbf{(1)}$$

Where x is the distance from the origin in the horizontal axis, y is the distance from the origin in the vertical axis and σ^2 represent the variance which determine the amount of smoothing.

Fig. 3. Liver segmentation

C. *Wavelet Feature Extraction*

Discrete Wavelet Transform (DWT) [18] is a method to transform image pixels into wavelets, which are then used for wavelet-based compression and coding. DWT defined as:

$$W_{\varphi}(j_o k) = \frac{1}{\sqrt{M}} \sum_k f(x) \varphi_{j_{o,k}}(x) \quad \textbf{(2)}$$

$$W_{\psi}(\mathrm{j}, k) = \frac{1}{\sqrt{M}} \sum_k f(x) \psi_{jk,}(x) \quad \textbf{(3)}$$

where $\varphi_{j_{o,k}}(x) and\ \psi_{jk,}(x)$ are function of discrete variable x=1,2,3….M (DWT) [12] algorithm is carried out to extract characteristics from an image on various scales proceeding by successive high pass($h_1(n)$) and low pass($h_1(n)$) filter coefficients. Filters are used separately on columns and rows to obtain 2-D transformation of image $l(m,n)$ of size $N\,X\,N$ which have high and low frequency respectively. The wavelet coefficients are the successive continuation of the approximation and detail coefficients. The basic wavelet feature extraction procedure consists of:

a) Load the Segmented liver image
b) Apply wavelet packet decomposition(WPD) function to compute the approximation coefficients matrix and detail coefficients matrices (horizontal, vertical, and diagonal, respectively) obtained by a wavelet decomposition (high pass and low pass filters) of the vector X using Daubechies wavelet filter.
c) Apply wavelet packet coefficients function to return associate coefficient with the node N of the wavelet packet tree T. The wavelet pocket coefficients are defined as [19].

$$w_o^o(l) = x_l \qquad l = 0, \ldots N-1 \quad \textbf{(3)}$$

$$w_j^{2p+1}(l) = \sum_k hk - 2l \;\; w_{j-1}^n(k) \;\; l = 0 \ldots., N2^{-j} - 1 \quad \textbf{(4)}$$

Where j=1,2….J; J=$log_2 N, w_j^p$ is transform coefficient parallel to wavelet pocket function which has relative support size 2^j, frequency $p2^j\ and\ located\ at\ l2^j$. The following features were computed:

1. Compute the energy density using the following formula

$$e = \sum \infty n = -\infty |X(n)|2 \quad \textbf{(5)}$$

2. Compute Kurtosis (is a measure of how outlier-prone a distribution is) using the following equation.

$$k = \frac{E(X-\mu)^4}{\sigma^4} \quad \textbf{(6)}$$

where μ is mean of x, σ is standard deviation of X and E(t) expected value of quantity t.

3. Compute Skewness (it is a measure of the asymmetry of the data around the sample mean) using the following equation. The skewness is defined as:

$$s = \frac{E(X-\mu)^3}{\sigma^3} \quad \textbf{(7)}$$

where μ is the mean of x, σ is standard deviation of the X and E(t) represents the expected value of the quantity t.

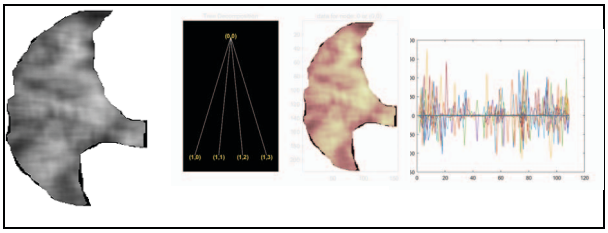

Fig. 4. Wavelet Feature extraction

D. *HCC Classification*

In order to develop an HCC and non-HCC classification model, extracted feature dimensions of the input vector, combined with laboratory data, were utilized for training and testing. In this model, a 10-fold cross validation [20] was used to avoid over-fitting. The data set consisted of 26 patients' CT abdomen images and their laboratory data. The experiments were performed with CT images, laboratory data and classification, and a combination of feature extraction and laboratory data. The extracted features and laboratory data were tested with SVM by using different kernel functions. To simulate experiment results using an SVM classifier, the following four stages were followed: (1) input variable selection, (2) data pre-processing and partitioning, (3) the setting of model parameters, and (4) model implementation [21]. In the first experiment, the SVM took a set of features, $h_N = [e^T\ k^T\ s^T]$ as input data and predicted HCC and non-HCC classes from each feature vector. In the second experiment, laboratory data was used to discriminate between HCC and non-HCC cases. In the third experiment, we combined the CT image with the laboratory data. In this mode, the SVM drew a hyper plane that was isolated into two classes, namely, HCC and non-HCC. The hyper plane can be taken by following the equation where W is the normal vector to the hyper plane.

$$\boldsymbol{g(x) = W^t(h_N) + W_0 = 0} \qquad (8)$$

The SVM is used to train different sample features. This training classifier model can assign classes to unknown feature vectors. The SVM can perform both linear and non-linear classification. Kernel function can significantly improve the SVM's performance. The experiments were performed with four kernel functions, namely, linear, polynomial, radial-based function or Gaussian polynomial kernel and Sigmoid or Hyperbolic Tangent Kernel, as given below:

Linear Kernel: $\mathrm{k}(\mathrm{h_N}, \mathrm{h'_N}) = \mathrm{h_N^T}, \mathrm{h'_N} + \mathrm{C}$ **(9)**

where C is the optimal constant.

Polynomial Kernel:

$\mathrm{k}(\mathrm{h_N}, \mathrm{h'_N}) = (\gamma \mathrm{h_N^T h'_N} + \mathrm{C})$ **(10)**

where γ and C are adjustable constant and d is the degree of the polynomial.

Gaussian Polynomial Kernel:

$\mathrm{k}(\mathrm{h_N}, \mathrm{h'_N}) = \exp(-\gamma||\mathrm{h_N} - \mathrm{h'_N}||^2)\ \gamma > 0$ **(11)**

where γ is, a positive parameter controlling the radius.

Hyperbolic Tangent (Sigmoid) Kernel:

$$\mathrm{k}(\mathrm{h_N}, \mathrm{h'_N}) = \tanh(\gamma \mathrm{h_N^T h'_N} + \mathrm{C})\gamma > 0 \textbf{ (12)}$$

IV. Experiment Results and Discussion

The experiments and analysis have been performed using the abdomen CT images and laboratory data of 32 patients, acquired from Crosshouse Hospital, Kilmarnock. The acquired images were in a DICOM format of size 512 X 512. In the enhancement phase, different image enhancement techniques were applied for the analysis, evaluation, and comparisons as shown in Figure-2. The comparison was carried out based on three parameters, namely, Entropy, Mean Square Error(MSE), Root Mean Square Error (RMSE) and Mean Square Error (MSE). These parameters were utilized as the target measures for the performance evaluation of applied enhancement methods. According to the assessment, the results of the normal and enhanced images are shown in Table-1. CLAHE achieved the minimum MSE of 0.19 and highest entropy value of 7.39, and remained the best method. In the segmentation phase, as shown in Figure-3, the result of the proposed algorithm is compared with the manual segmentation done by experts. The automatic and manual segmentations of liver and HCC were evaluated and compared with the following measures [22].

A. Performance Measures

Several performance tools were used to evaluate the performance of the various classifiers, namely, accuracy, sensitivity, specificity and Area Under Curve (AUC), in classifying a liver tumor [23]. Each of them was used to measure different aspects of the classifiers' performance. Accuracy evaluates the overall effectiveness of the classifier, sensitivity and specificity estimates the classifiers' performance in different categories.

In our case, sensitivity measured the percentage of HCC patients while specificity measured the percentage of non-HCC patients correctly. AUC determined the common measures of sensitivity and specificity.

$$\mathrm{Accuracy}(\%) = \frac{(\mathbf{TP+TN})}{(\mathbf{TP+FN+TN+FP})}\mathrm{X100} \quad \textbf{(13)}$$

$$\mathrm{Sensitivity}(\%)\mathrm{TPR} = \frac{\mathrm{TP}}{(\mathrm{FN+TP})}\mathrm{X100} \quad \textbf{(14)}$$

$$\mathrm{Specificity}(\%)\mathrm{TNR} = \frac{\mathrm{TN}}{(\mathrm{TN+FP})}\mathrm{X100} \quad \textbf{(15)}$$

$$\mathbf{AUC}(\%) = \frac{\mathbf{1}}{\mathbf{2}}\left(\frac{\mathbf{TP}}{(\mathbf{TP+FN})} + \frac{\mathbf{TN}}{(\mathbf{TN+FP})}\right)\mathbf{X100} \quad \textbf{(16)}$$

Positive Predictive Value or Precision=TP/(TP+FP) **(17)**

$$\textbf{Negative Predictive Value or Precision} = \frac{\mathbf{TN}}{\mathbf{TN+FN}} \textbf{ (18)}$$

Definitions of True and False positive/negative in case of HCC and Non -HCC [20] as follows:

- True positive(TP): HCC people correctly diagnosed as HCC
- False positive(FP): Non-HCC people incorrectly identified as HCC
- True negative(TN): Non-HCC people correctly identified as Non-HCC
- False negative(FN): Non-HCC people incorrectly identified as HCC

Table 1- Image Enhancement Results

Methods	Entropy	Mean Square Error (MSE)	Root Mean Square Error (RMSE)
Histogram	7.33	0.22	0.46
CLAHE	7.39	0.19	0.40

Table 2- Experiment Results Setup

Image Features	Lab Feature	Out Put	Test Mode
E1,E2,E3,E4, K1,K2,K3,K4, S1, S2, S3, S4 E=Energy K=Keratosis S=Entropy	AFP, ALT	Diagnosis: HCC-Yes, HCC-No	10 -Fold cross validation

Table 3- Cross-Validation Summary

Classifier	Support Vector Machine(SVM)
Correctly Classified Instances 23	88.4615 %
Incorrectly Classified Instances 3	11.5385 %
Kappa statistic	0
Mean absolute error	0.1154
Root mean squared error	0.3397
Relative absolute error	49.7449 %
Root relative squared error	102.9716 %

Table 4- Detailed Accuracy by Class-SVM

TP Rate	FP Rate	Precision	Recall	F-Measure	ROC	Class
0	0	0	0	0	0.38	HCC-N
1	1	0.88	1	0.94	0.78	HCC-Y
0.88	0.88	0.78	0.88	0.83	0.74	Weight

Table 5- Cross-Validation Summary

Classifier	MLP
Correctly Classified Instances 23	87.45%
Incorrectly Classified Instances 3	12.5385 %
Kappa statistic	0
Mean absolute error	0.15
Root mean squared error	0.35
Relative absolute error	68.14 %
Root relative squared error	105.06 %

Table 6- Detailed Accuracy by Class-MLP

TP Rate	FP Rate	Precision	Recall	F-Measure	ROC	Class
0.33	0.21	0.17	0.33	0.22	0.65	HCC-N
0.78	0.66	0.90	0.78	0.84	0.44	HCC-Y
0.73	0.62	0.81	0.73	0.77	0.47	Weight

Table 7- Detailed Accuracy by Class

TP Rate	FP Rate	Precision	Recall	F-Measure	ROC	Class
0	0	0.2	0.1	0	0.32	HCC-N
1	1	0.85	1	0.93	0.63	HCC-Y
0.88	0.88	0.78	0.88	0.83	0.59	Weight

Table 8- Cross-Validation Summary

Classifier	Logistic Regression
Correctly Classified Instances 19	73.0769 %
Incorrectly Classified Instances 7	26.9231 %
Kappa statistic	0.08
Mean absolute error	0.2448
Root mean squared error	0.4783
Relative absolute error	105.5556 %
Root relative squared error	144.9776 %

Table 9- Detailed Accuracy by Class-Logistic Regression

TP Rate	FP Rate	Precision	Recall	F-Measure	ROC	Class
0.333	0.217	0.167	0.333	0.222	0.647	HCC-N
0.783	0.667	0.9	0.783	0.837	0.444	HCC-Y
0.731	0.615	0.815	0.731	0.766	0.468	Weight

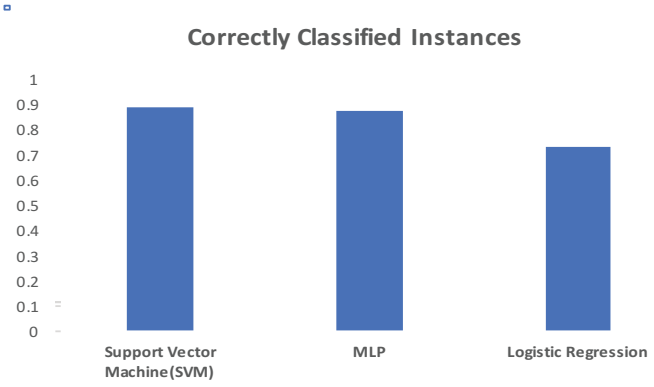

Fig. 5. Classifiers Accuracy Comparision

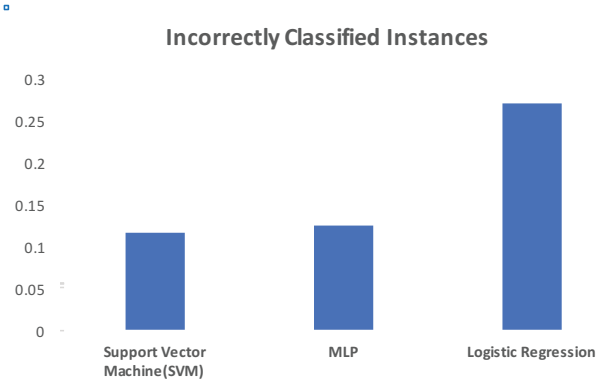

Fig. 6. Classifiers inaccuracy Comparision

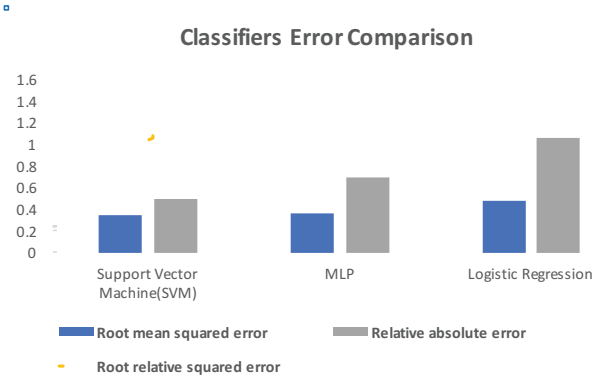

Fig. 7. Classifiers Error Comparision

The simulation results are depicted in Tables 1-5 and Figs 5-7. It can be seen that the highest correctly classified accuracy of 88.46 %, was achieved using SVM with a linear kernel as shown in fig-5. The second-best classifier was MLP with 87.45%, as shown in Table 5. The lowest accuracy was achieved with logistic regression as shown in Table 8. The classifiers error such as root mean squared error, relative absolute error, and root relative squared error are shown in fig-7. It is to be noted that a combination of wavelet feature extraction and lab markers remained the best choice to detect, diagnose and classify HCC disease.

V. Conclusion

In this research, wavelet feature extraction is implemented for the first time using 3D medical CT scan image data for HCC diagnosis. The performance of HCC and Non-HCC classification together with 3D liver wavelet features and lab markers were evaluated. The performance evaluation was done by considering the accuracy, sensitivity, specificity and AUC by applying a 10-fold cross validation [25]. For each classifier, we simulated different experiments e.g., tuning the parameters of the model, with a view to acquiring the optimal trade-off between classification accuracy and conformity of results. Different state of the art machine-learning classifiers, such as SVM, logistic regression and Multilayer Perceptron (MLP), were used to assist in the early diagnosis of HCC. The simulation results showed that SVM performed the best with the fusion of lab markers and wavelet features as compared to MLP and logistic regression. In addition, the experimental results demonstrated that the wavelet features in combination with laboratory data outperformed the state-of-the-art feature extraction methods. Consequently, it is evident that our proposed CAD system is effective and accurate in segmentation, feature extraction and classification of HCC. For future work, a comprehensive evaluation and clinical validation is required with larger datasets to verify system scalability and robustness. The proposed system can also be expanded to utilize Positron Emission Tomography (PET), Magnetic Resonance Imaging (MRI) datasets, and for the diagnosis of a wide range of diseases across body systems.

Acknowledgments

This research is funded by the University of Stirling (Scotland, UK), and Ucare Foundation, as part of a collaborative PhD IMPACT project. The authors are grateful to the anonymous reviewers for their insightful comments and suggestions, which helped improve the quality of this paper.

References

[1] A. J. Roth, "http://www.targetedonc.com/publications/hcc-monitor/2015/hcc-april-2015/diagnosis-treatment-of-hcc-remains-challenging," 18 May 2015. [Online].

[2] M. N. B. A.-H. A. C. Y. J. A. T. J. A. M. A. S. L. W. M. L. Amit G. Singal, "Detection of hepatocellular carcinoma at advanced stages among patients in the HALT-C trial: Where did surveillance fail," *American Journal of Gastroenterology,* vol. 108, no. 3, pp. 425-432.

[3] S. K. A. M. B. S. C. J. Srinivasa Rao, "OBJECT-BASED IMAGE ENHANCEMENT TECHNIQUE FOR GRAY SCALE IMAGES," *International Journal of Advanced Information Technology (IJAIT),* vol. 04, no. 03, June 2014.

[4] D. S. R. J. D. F. Roman Lerman, "Contrast enhancement of soft tissues in Computed Tomography".

[5] V. M. Georgieva, "An Approach for Computed Tomography Images Enhancement," *MEDICINE TECHNOLOGY,* vol. 2, no. 98, 2010.

[6] A. K. Abouzar Zareei, "Liver segmentation with new supervised method to create initial curve for active contour," *Elsevier-Computers in Biology and Medicine ,* pp. 139-150, May 2016.

[7] K. A. A. K. Abouzar, "Liver segmentation with new supervised method to create initial curve for active contour,," *Computers in Biology and Medicine,* vol. 5, pp. 139-150, 2018.

[8] A. F. M. A. E. E. H. a. H. H. Abdalla Mostafa, "Artificial Bee Colony Based Segmentation for CT Liver Images," *Springer-Medical Imaging in Clinical Applications,,* pp. 409-429, 2016.

[9] L. N. L. Z. H. G. Z. W. Z. J. D. Y. Huang W, "Liver tumor detection and segmentation using kernel-based Extreme Learning Machine.," in *IEEE Engineering in Medicine and Biology Society*, 2013.

[10] R. B. P. R. A. Shishir Maheshwari, "Automated Diagnosis of Glaucoma Using Empirical Wavelet Transform and Correntropy Features Extracted from Fundus Images," in *Journal of Biomedical and Health Informatics*, 2016.

[11] Q. C. S. Z. Minrong Zhao, "A method of image feature extraction using wavelet transforms," in *ICIC'09 Proceedings of the 5th international conference on Emerging intelligent computing technology and applications*, 2009.

[12] R. M. R. S.S. Kumar, " An automatic computer-aided diagnosis system for liver tumours on computed tomography images ☆," *Computers & Electrical Engineering,* vol. 39, no. 5, p. 1516–1526, 08 02 2013.

[13] I. K. V. A. N. S. N. Stavroula G. Mougiakakou, “Differential diagnosis of CT focal liver lesions using texture features, feature selection and ensemble driven classifiers,” *Artificial Intelligence in Medicine- Elsevier ,* pp. 25-37, 2007.

[14] T. Z. S. Busayarat, "Lung Surface Classification on High-Resolution CT using Machine Learning".

[15] W. J. R. J. L. J. M. W. V. P. W. a. R. M. S. Marius George Linguraru*, “Tumor Burden Analysis on Computed Tomography by Automated Liver and Tumor Segmentation,” vol. VOL. 31, 2012 .

[16] A. H. J. L. N. H. A. A. S. U. S. M. A. S. Z. U. H. Liaqat Ali, A Novel Fully Automated Liver and HCC Tumor Segmentation System Using Morphological Operations, China : Springer, 2016, pp. 240-250.

[17] S. M. A. A. Garima Yadav, "Multi-domain Image Enhancement of Foggy Images Using Contrast Limited Adaptive Histogram Equalization Method," in *Proceedings of the International Conference on Recent Cognizance in Wireless Communication & Image Processing*.

[18] B. Furht, "Discrete Wavelet Transform (DWT)," p. 188, 2008.

[19] N. Rajpoot, "Texture classification using discriminant wavelet packet subbands," in *he 2002 45th Midwest Symposium on Circuits and Systems, 2002. MWSCAS-2002.*, 2002.

[20] S. B. Zrimec, "Lung Surface Classification on High-Resolution CT using Machine Learning," in *11th Mediterranean Conference on Medical and Biomedical Engineering and Computing*, 2007.

[21] N. L. Weimin Huang, Z. Lin, G.-B. Huang, W. Zong, J. Zhou and Y. Duan, "Liver tumor detection and segmentation using kernel-based extreme learning machine," Osaka, 2013.

[22] M. R. J. Kumar S.S., “An automatic computer-aided diagnosis system for liver tumours on computed tomography images,” vol. 39 , 2013.

[23] Sharifah Hafizah Sy Ahmad Ubaidillah, “Classification of Liver Cancer using Artificial Neural Network and Support Vector Machine,” 2014 .

[24] M. M. S. M. R. M. ·. M. I. B. Saripan, "Review of liver segmentation and computer assisted detection/diagnosis methods in computed tomography," *Artificial Intelligence Review,* 20 03 2017.

[25] F. D. S. Federica Ciocchetta, "Machine learning methods to understand hepatocellular carcinoma pathology".